NJC
New Journal of Chemistry
A journal for new directions in chemistry

This article can be cited before page numbers have been issued, to do this please use: W. Wang, L. Huai, X. Wang, K. Jiang, H. Shen, H. Gao, M. Fang and J. Cui, *New J. Chem.*, 2020, DOI: 10.1039/D0NJ01969K.

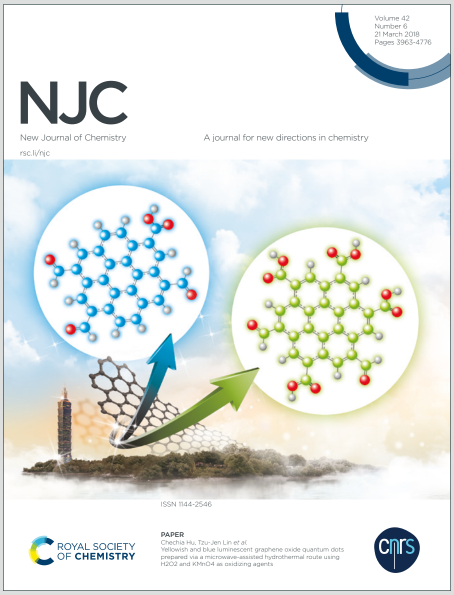

ROYAL SOCIETY OF CHEMISTRY

rsc.li/njc

View Article Online
DOI: 10.1039/D0NJ01969K

Structures, magnetic refrigeration and single molecule-magnet behavior of five rhombus-shaped tetranuclear Ln(III)-based clusters

Wen-Min Wang,[a,b] Lei Huai,[a] Xi-Wen Wang,[a] Kai-Jun Jiang,[b] Hai-Yun Shen,[b] Hong-Ling Gao,[b] Ming Fang, *[c] Jian-Zhong Cui*[b]

Abstract

A serie of coplanar tetranuclear Ln(III)-based clusters, namely [$Ln_4(acac)_4(L)_6(\mu_3$-$OH)_2$]·[solvent] (Ln = Eu (**1**), Gd (**2**), Tb (**3**), Dy (**4**) and Er (**5**)), have been synthesized by using an 8-hydroxyquinoline Schiff base ligand (HL = 5-(2-thenylidene)-8-hydroxylquinoline) and acetylacetone. The structures and magnetic properties of them have been completely characterized. The structures determinations show that clusters **1**-**5** are isostructural with a rhombus-shaped Ln_4 core. The magnetic studies reveal that Gd_4 cluster (**2**) displays cryogenic magnetocaloric effects with maximum $-\Delta S_m$ value of 22.09 J kg^{-1} K^{-1} at 2.5 K and ΔH = 7.0 T; while ac susceptibility measurements show that single molecule-magnet behavior occurs for Dy_4 cluster (**4**) with the anisotropic barrier ($\Delta E/k_B$) of 75.01 K. Interestingly, more than one maxima out-of-phase *ac* signals (χ'') were observed in **4**, suggesting the operation of multiple magnetic relaxation processes in **4**. In addition, the solid state luminescence properties reveal that clusters **1**, **3**, and **4** display the characteristic lanthanum luminescence at room temperature.

---

[a] *Department of Chemistry, Taiyuan Normal University, Jinzhong 030619, China*

[b] *Department of Chemistry, Tianjin University, Tianjin, 300072, China*

[c] *Department of Chemistry, Hebei Normal University of Science & Technology, Qinhuangdao 066004, China*

Corresponding Authors E-mail：cuijianzhong@tju.edu.cn, fangmingchem@163.com.

View Article Online
DOI: 10.1039/D0NJ01969K

Introduction

Polynuclear lanthanide-based clusters have attracted much attention and got a rapid development due to the unabated interest in magnetocaloric effects, single-molecule magnets (SMMs), luminescence properties and catalytic properties of them during the past two decades.[1-4] Among these applications, the investigation of Ln(III)-based SMMs have been of much more interest, not only because of their interesting magnetic properties but also owing to the rapid development of molecular magnetism materials.[5] Since the first Ln(III)-based SMM, namely $[Pc_2Tb]^{-}$, has been synthesized by Ishikawa group in 2003,[6] the Ln(III)-based SMMs have experienced fast development and many of them with intriguing magnetism have been reported.[7] Tong, Zheng and Layfield groups did original and excellent works in design and synthesis of Ln(III)-based SMMs.[8] In 2016, Tong group reported a Dy(III)-based SMM displaying excellent magnetic property with the effective energy barrier U_{eff} as large as 1025 K;[9] shortly afterwards, the group of Zheng reported a nearly perfect pentagonal bipyramidal Dy compound with the larger U_{eff} of 1815 K.[10] In 2018, the record of effective energy barrier (U_{eff}) has been broken by the group of Layfield, a dysprosium metallocene cation $[(Cp^{i/Pr5})Dy(Cp^{*})]^{+}$ with the largest U_{eff} of 2219 K was reported, setting a the record in this field of Ln(III)-based SMMs.[11] For polynuclear lanthanide-based SMMs, lots of interesting and well works were reported by the group of Tang.[12] Among these studies of polynuclear Ln(III)-based clusters, Dy_3, Dy_4 and Dy_6 clusters with outstanding SMMs behaviors were reported widely.[13] These studies attracted and promoted a rapid development of polynuclear Ln(III)-based SMMs.

For another research field of polynuclear lanthanide-based clusters, the research of magnetic refrigerant was one of frontier hot. Magnetic refrigeration depends on the magnetocaloric effect (MCE), which represents isothermal magnetic entropy change (ΔS_m) and adiabatic temperature (ΔT_{ad}) in change of applied magnetic field.[14] Researches show that the Gd(III) ion is the best and unique candidate for constructing magnetic refrigeration materials.[15] In view of this, lots of Gd(III)-based clusters showing well and excellent magnetic refrigeration properties have been

View Article Online
DOI: 10.1039/D0NJ01969K

reported in these years.[16] In 2014, Long's group reported an unprecedented Gd_{104} cluster with a large magnetic entropy change ($-\Delta S_m$) of 46.9 J kg $^{-1}$ K $^{-1}$ (T = 2.0 K and ΔH = 7 T).[17] In 2015, a Gd_{60} nanocage with larger magnetic entropy change of $-\Delta S$ = 66.5 J kg $^{-1}$ K $^{-1}$ (T = 3K, ΔH =7 T) was reported by Zhao group.[18] It seems that the high nuclear Gd(III)-based clusters can get larger $-\Delta S$ values and excellent magnetic refrigeration properties.

According to the above, although many exciting works based on the Ln(III)-based mononuclear compounds or polynuclear clusters have been reported, there is still a challenge for designing and constructing Ln(III)-based polynuclear clusters with outstanding magnetic properties.[19] In these years, our work mainly focus on the study of magnetic refrigeration and single molecule magnets of Ln(III)-based polynuclear clusters, and some Ln_4 or Ln_6 (Ln^{III} = Gd and Dy) clusters show well magnetic properties.[20] Continue the previous work, in this paper, we have designed and synthesized a series of rhombus-shaped tetranuclear lanthanide [Ln_4] clusters constructed by 8-hydroxyquinoline Schiff base and acetylacetone ligands (Scheme 1). The structures and magnetic properties of them have been systematically studied in this work.

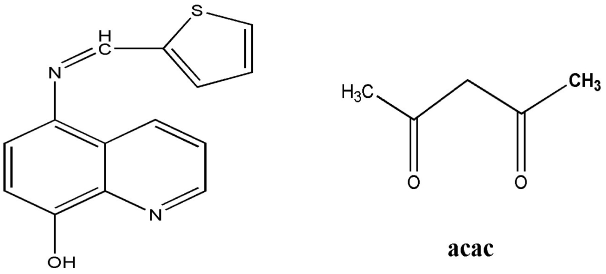

Scheme 1 The structures of HL (left) and acac (right).

Experimental Section

Materials and Methods

All chemicals, rare earth salts and solvents used for the syntheses were reagent grade without further purification. The β-diketionate salts $Ln(acac)_3\cdot 2H_2O$ (Ln (III) = Eu, Gd, Tb, Dy and Er) were synthesized according to the method in the literature.[21] The 8-hydroxyquinoline Schiff base ligand HL were synthesized according to the already

View Article Online
DOI: 10.1039/D0NJ01969K

reported methods.[22]

Elemental analyses (EA) for C, H and N were performed on a Perkin-Elmer 240 CHN elemental analyzer. IR spectra were recorded in the range of 400−4000 cm^{-1} with a Bruker TENOR 27 spectrophotometer using a KBr pellet. PXRD data were examined on a Rigaku Ultima IV instrument with Cu Kα radiation (λ = 1.54056 Å), with a scan speed of 10° min^{-1} in the range of $2\theta = 5 - 50°$. Luminescence properties were recorded on an F-4500 FL spectrophotometer with a xenon arc lamp as the light source.

Synthesis section

Synthesis of clusters 1-5. Ln(acac)$_3$·2H$_2$O (0.03 mmol) (Ln = Eu (**1**), Gd (**2**), Tb (**3**), Dy (**4**) and Er (**5**)) and HL (0.03 mmol) were dissolved in acetonitrile / CH$_2$Cl$_2$ solution (15 mL /5 mL). Then the mixture solution was stirred for about 4 h at 70 ℃. Finally, the solution was filtered and kept in the dark and concentrated slowly by evaporation at 4 ℃. After about 5 days, light-colored yellow block crystals suitable for single crystal X-ray diffraction analysis were isolated.

[Eu$_4$(acac)$_4$(L)$_6$(μ_3-OH)$_2$]·CH$_3$CN (**1**). Yield: 32% (based on Eu). Elemental analysis (%) calcd for $C_{106}H_{87}Eu_4N_{13}O_{16}S_6$ (F_w = 2599.08): C, 48.94; H, 3.35; N, 7.00. Found: C, 49.08; H, 3.29; N, 6.91. IR (KBr, cm^{-1}): 3683 (m), 1560 (s), 1511 (s), 1464 (s), 1395 (m), 1312 (s), 1251 (w), 1093 (m), 1016 (w), 837 (m), 786 (m), 705 (m).

[Gd$_4$(acac)$_4$(L)$_6$(μ_3-OH)$_2$]·CH$_3$CN (**2**). Yield: 35% (based on Gd). Elemental analysis (%) calcd for $C_{106}H_{87}Gd_4N_{13}O_{16}S_6$ (F_w = 2620.24): C, 48.55; H, 3.32; N, 6.95. Found: C, 48.48; H, 3.46; N, 7.09. IR (KBr, cm^{-1}): 3681 (m), 1558 (s), 1510 (s), 1465 (s), 1395 (m), 1310 (s), 1250 (w), 1093 (m), 1016 (w), 836 (m), 785 (m), 705 (m). **[Tb$_4$(acac)$_4$(L)$_6$(μ_3-OH)$_2$]·CH$_3$CN** (**3**). Yield: 31% (based on Tb). Elemental analysis (%) calcd for $C_{106}H_{87}N_{13}O_{16}S_6Tb_4$ (F_w = 2626.92): C, 48.42; H, 3.31; N, 6.93. Found: C, 48.56; H, 3.48; N, 7.05. IR (KBr, cm^{-1}): 3684 (m), 1560 (s), 1510 (s), 1464 (s), 1397 (m), 1313 (s), 1250 (w), 1095 (m), 1013 (w), 835 (m), 788 (m), 706 (m).

[Dy$_4$(acac)$_4$(L)$_6$(μ_3-OH)$_2$]·CH$_3$CN (**4**). Yield: 45% (based on Dy). Elemental analysis (%) calcd for $C_{106}H_{87}Dy_4N_{13}O_{16}S_6$ (F_w = 2641.24): C, 48.16; H, 3.29; N, 6.89. Found: C, 48.27; H, 3.15; N, 6.80. IR (KBr, cm^{-1}): 3628 (m), 1598 (s), 1512 (s), 1463 (s), 1397(s), 1313 (s), 1252 (w), 1093 (s), 1016 (w), 921 (w), 838 (m), 786 (s), 707 (s).

[Er$_4$(acac)$_4$(L)$_6$(μ_3-OH)$_2$]·2CH$_3$CN (**5**). Yield: 31% (based on Er). Elemental analysis (%) calcd for $C_{108}H_{90}Er_4N_{13}O_{17}S_6$ (F_w = 2701.33): C, 47.98; H, 3.33; N, 6.74. Found: C, 47.68; H, 3.45; N, 6.98. IR (KBr, cm^{-1}): 3630 (m), 1598 (s), 1514 (s), 1465 (s), 1397(s), 1315 (s), 1250 (w), 1095 (s), 1015 (w), 920 (w), 837 (m), 786 (s), 705 (s).

Magnetic measurements

Magnetic measurements were performed with a Quantum Design MPMS-XL7 and a PPMS-9 ACMS magnetometer in temperature ranges 2.0–300 K. The polycrystalline samples were grounded and placed in a gel capsule. A small amount of eicosane was used to avoid movement of the sample during the measurement. Diamagnetic corrections for the compounds were estimated using Pascal's constants, and magnetic data were corrected for diamagnetic contributions of the sample holder.[23] Magnetic data were fitted using the 0rigin 8.0 software.

Crystal Structure Determinations

Single crystal X-ray diffraction data of **1**−**5** were collected on a computer-controlled Bruker P4 CCD area detector diffractometer, equipped with confocal monochromatized Mo Kα radiation with a radiation wavelength of 0.71073 Å using the ω-φ scan technique. The structures were solved by direct methods and refined with a full-matrix least-squares technique based on F^2 using the SHELXS-2016 and SHELXL-2016 programs.[24] Anisotropic thermal parameters were assigned to all non-hydrogen atoms. The crystals of **1**-**5** were measured as soon as they were isolated from the reaction solvents, hence, some disordered free solvent molecules were still existed in the crystal structures. Some free solvent molecules were removed via "SQUEEZE" due to their extreme disorder which can not be solved. Crystallographic data and structural refinement parameters are listed in Table 1. The important bond lengths (Å) and angles (°) for **1**–**5** are given in Tables S1−S5 (in ESI). CCDC (**1**; 1585585, **2**; 1585587, **3**; 1585588, **4**; 1585589, **5**; 1585590) contain the supplementary crystallographic data for this paper. These data can be obtained free of charge from The Cambridge Crystallographic Data Centre.

View Article Online
DOI: 10.1039/D0NJ01969K

Table 1. Crystallographic Data and Structure Refinements for clusters **1-5.**

Compounds	**1**	**2**	**3**	**4**	**5**
formula	$C_{106}H_{87}Eu_4N_{13}O_{16}S_6$	$C_{106}H_{87}Gd_4N_{13}O_{16}S_6$	$C_{106}H_{87}N_{13}O_{16}S_6Tb_4$	$C_{106}H_{87}Dy_4N_{13}O_{16}S_6$	$C_{108}H_{90}Er_4N_{13}O_{17}S_6$
Mr (g mol^{-1})	2599.08	2620.24	2626.92	2641.24	2701.33
T (K)	113.15	113.15	113.15	113.15	113.15
cryst syst	Monoclinic	Monoclinic	Monoclinic	Monoclinic	Monoclinic
Space group	$P2_1/n$	$P2_1/n$	$P2_1/n$	$P2_1/n$	$P2_1/n$
a (Å)	15.148(3)	15.115(5)	15.1763(9)	15.194(3)	15.189(2)
b (Å)	12.762(2)	12.699(4)	12.7802(7)	12.779(2)	12.7422(19)
c (Å)	28.486(4)	28.477(9)	28.3434(16)	28.304(5)	28.246(4)
α (°)	90	90	90	90	90
β (°)	101.850(9)	102.116(8)	102.5790(10)	102.649(4)	102.961(2)
γ (°)	90	90	90	90	90
V (Å^3)	5389.5(15)	5344(3)	5365.4(5)	5362.3(15)	5327.3(14)
Z	2	2	2	2	2
cryst size (mm^3)	0.20 x 0.18 x 0.12	0.20 x 0.18 x 0.12	0.20 x 0.18 x 0.12	0.20 x 0.18 x 0.12	0.20 x 0.16 x 0.12
Dc (g cm^{-3})	1.602	1.628	1.626	1.635	1.684
μ (mm^{-1})	2.480	2.636	2.790	2.941	3.307
R_{int}	0.0597	0.0932	0.0238	0.0356	0.1515
limiting indices	-17<=h<=17	-17<=h<=17	-18<=h<=15	-19≤ h ≤19	-18<=h<=18
	-15<=k<=15	-14<=k<=15	-15<=k<=15	-16<=k<=16	-15<=k<=15
	-33<=l<=33	-32<=l<=33	-31<=l<=33	-23<=l<=36	-33<=l<=33
reflns collected	42915	43749	44596	53324	38038
params	773	726	773	726	735
GOF on F^2	1.090	1.084	1.084	1.073	1.013
R_1, wR_2 [$I>2\sigma(I)$]	0.0648, 0.2021	0.0763, 0.1667	0.0339, 0.0982	0.0302, 0.0802	0.0357, 0.0813
R_1, wR_2 (all data)	0.0755, 0.2106	0.1232, 0.1871	0.0385, 0.1010	0.0370, 0.0835	0.0463, 0.0832

Results and discussion

Crystal structures of clusters 1–5

Single-crystal X-ray diffraction analysis reveal that clusters **1–5** are isomorphous and crystallize in the monoclinic system space group $P2_1/n$ with $Z = 2$, so, the structure of Dy(III)-based cluster **4** is selected and described in detail. As shown in Fig. 1, the molecular structure of **4** is mainly composed of four Dy^{3+} ions, four acac$^-$, six Schiff base ligand L$^-$ and two μ_3-OH. Each central Dy^{3+} is eight coordinated, and their coordination polyhedrons can be described as a distorted square-antiprismatic geometry (Table S6), which was identified by using Shape 2.0 software. The Dy1 atom connected by two N atoms (N1 and N3) and six O atoms (O1, O2, O3, O4, O5, and O8), while the central Dy2 atom is connected by one N atom (N5) and seven O atoms (O1a, O2a, O3,

View Article Online
DOI: 10.1039/D0NJ01969K

O6, O7, O8, and O8a) with a O_7N coordination environment (Fig. S1). The Schiff base ligand L$^-$ adopts a μ_2-O coordination mode to connect two central Dy^{3+} ions, and the acac$^-$ adopts a bidentate chelate coordination mode to connect each central Dy^{3+} ion (Fig. 2). The core four Dy^{3+} ions are bridged by six μ_2-O and two μ_3-O atoms forming a rhombus-shaped [Dy$_4$] (Fig. S2). In the Dy$_4$ core, the important bond lengths of Dy-N are in the range of 2.513(3)–2.548(3) Å, and Dy–O bond lengths are in the range of 2.301(2)-2.416(2) Å; and the O–Dy–O bond angles are in the range of 67.81(8)–144.61(9)°. These important bond lengths and bond angles are comparable to those of already reported Dy$_4$ clusters.[25] Furthermore, the adjacent Dy···Dy distances of **4** are 3.5381(8) and 3.8616(6) Å, and the bidiagonal Dy···Dy distances are 3.8114(9) and 6.3508(10) Å. The Dy2−Dy1−Dy2a and Dy1−Dy2−Dy1a angles are 118.178°and 61.822°.

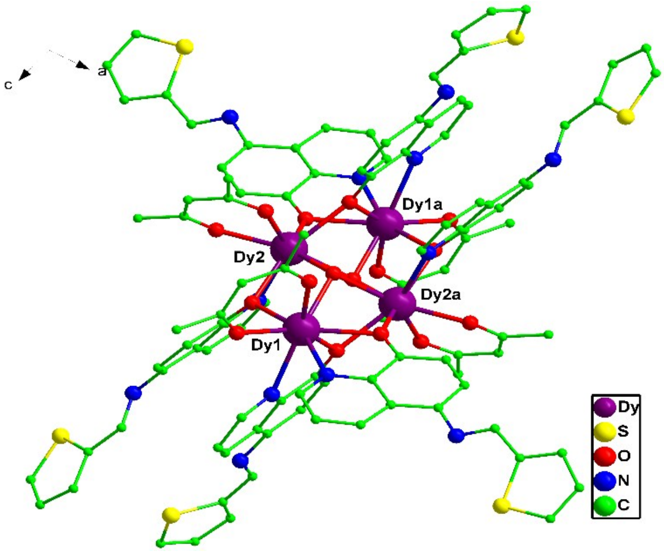

Fig. 1 Molecular structure for **4** (solvent molecules and all hydrogen atoms are omitted for clarity).

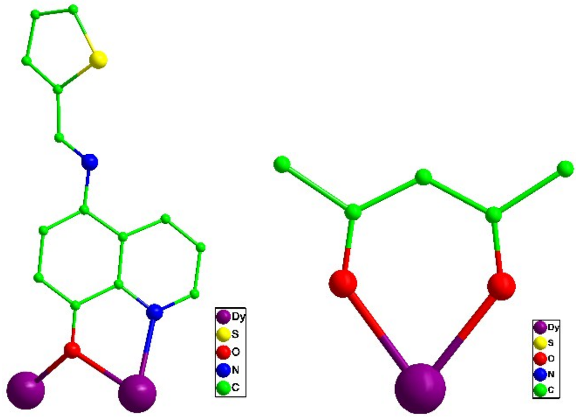

View Article Online
DOI: 10.1039/D0NJ01969K

Fig. 2 Coordination modes of HL (left) and acac$^-$ (right) in **4**.

Powder X-ray diffraction

To confirm the phase purity of Ln$_4$ clusters **1−5**, the polycrystalline products of **1−5** have been characterized by X-ray powder diffraction (PXRD) at room temperature (Fig. S3). The observed XRD patterns are in good agreement with the results simulated from the single crystal data, indicating the high purity of the synthesized polycrystalline samples **1-5**.

Luminescence properties

The solid-state luminescence properties of three Ln$_4$ clusters **1, 3** and **4** were measured at room temperature. As shown in Fig. S4, for cluster **1**, with the excitation of 295 nm, four characteristic peaks at 545, 592, 615 and 701 nm occur in the visible region, corresponding to the transitions of $^5D_1 \rightarrow ^7F_1$, $^5D_0 \rightarrow ^7F_1$, $^5D_0 \rightarrow ^7F_2$ and $^5D_0 \rightarrow ^7F_4$. These characteristic peaks are commonly observed in Eu^{III}-compounds.[26] Under the excitation of 296 nm, the emission spectra of cluster **3** exhibit the characteristic emissions of Tb^{III} ions, the emission band at 491, 546, 589 and 625 nm can be attributed to the $^5D_4 \rightarrow ^7F_6$, $^5D_4 \rightarrow ^7F_5$, $^5D_4 \rightarrow ^7F_4$ and $^5D_4 \rightarrow ^7F_3$ transitions, respectively.[27] Among them, the $^5D_4 \rightarrow ^7F_5$ transition is the strongest. Under the excitation of 290 nm, for cluster **4**, two characteristic peaks of Dy^{III} can be observed in the emission spectra, which belong to the transitions of $^4F_{9/2} \rightarrow ^6H_{15/2}$ (480 nm) and $^4F_{9/2} \rightarrow ^6H_{13/2}$ (576 nm).[28]

Magnetic properties

Magnetic studies were performed on polycrystalline samples of compounds **2-5**. Direct-current (dc) magnetic susceptibility studies of these compounds have been carried out in the in the temperature range 2.0–300 K with an applied magnetic field of 1000 Oe. The plots of $\chi_M T$ vs. T are shown in Fig. 3. At 300 K, the observed $\chi_M T$ products of **2-5** are 31.56 (**2**), 47.44 (**3**), 56.55 (**4**) and 45.95 (**5**) cm^3 K mol^{-1}, respectively; which are in good agreement with the theoretical values for four non-interacting Ln^{III} ions: four Gd^{III} ions ($^8S_{7/2}$, g = 2) give 31.52 cm^3 K mol^{-1} for **2**, four Tb^{III} ions ($^7F_6$, g = 3/2) give 47.28 cm^3 K mol^{-1} for **3**; four Dy^{III} ions ($^6H_{15/2}$, g = 4/3) give 56.68 cm^3 K mol^{-1} for **4** and four Er^{III} ions ($^4I_{15/2}$, g = 6/5) give 56.28 cm^3 K mol^{-1}

View Article Online
DOI: 10.1039/D0NJ01969K

for **5**. For cluster **2**, as the temperature is lowered, the $\chi_M T$ values stay almost constant in the temperature range 300−25 K and then drops rapidly to a minimum value of 15.83 cm^3 K mol^{-1} at 2.0 K, which indicate the presence of a weak antiferromagnetic interaction between the Gd^{III} ions.[29] For clusters **3**−**5**, upon lowering the temperature, the $\chi_M T$ values decrease slowly down to approximately 50 K then rapidly down to 2.0 K reaching values of 38.80 (**3**), 29.48 (**4**), and 25.60 cm^3 K mol^{-1} (**5**). The downtrend of $\chi_M T$ *vs*. T curves for **3-5** can be ascribed to the weak antiferromagnetic exchange between the Ln^{III} ions in the compounds system and/or the thermal depopulation of the Ln^{III} Stark sublevels.[30]

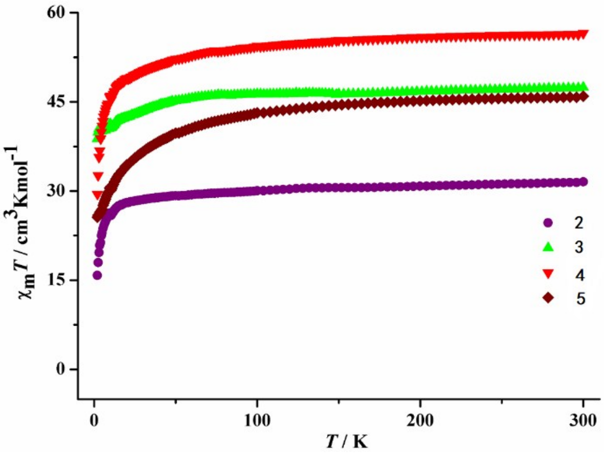

Fig. 3 Plots of $\chi_M T$ *vs*. T for compounds **2-5** under 1000 Oe dc field.

The field dependence of the magnetization for **2** was measured at 0−8.0 T between 2.0 and 10.0 K (Fig. 4). The M versus H curves display a gradual increase with the increasing field, and the M versus reach saturation values of 28.09 Nβ for **2** at 2.0 K and 8.0 T, which are extremely approximate with the theoretical value of 28.0 Nβ for four individual Gd(III) (S = 7/2, g = 2) ions. Because of the relatively high magnetic density and the isotropy of Gd^{III} ion of the polynuclear gadolinium-based cluster, the magnetocaloric effect of the Gd_4 cluster **2** was studied. Magnetic entropy changes ($-\Delta S_m$) of **2** are calculated from the M versus H data to evaluate the MCE, and the $-\Delta S_m$ values can be calculated by using the Maxwell equation: $\Delta S_m(T) = \int [\partial M(T, H)/\partial T]_H \, dH$.[31] As shown in Fig. 5, the maximum value of magnetic entropy change ($-\Delta S_m$) of

View Article Online
DOI: 10.1039/D0NJ01969K

are 24.46 J kg^{-1} K^{-1} at 2.0 K and ΔH = 7.0 T for **2**, which is smaller than the calculated values of 26.34 J kg^{-1} K^{-1} for four uncorrelated Gd^{III} (S = 7/2) ions based on the equation $-\Delta S_m = nR\ln(2S + 1)$ (where R is the gas constant, and S is the spin state). The difference of maximum $-\Delta S_m$ between the experimental and theoretical values for **2** are mainly due to the antiferromagnetic interaction in **2**.[32] The observed $-\Delta S_m$ value of **2** is smaller than the values of some Gd_4 clusters, however, the $-\Delta S_m$ value of **8** is bigger than other Gd_4 compounds (Table 2).[33-35]

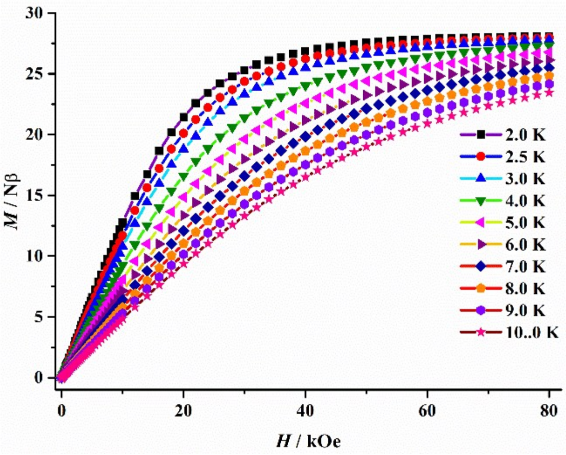

Fig. 4 M versus H plots for **2** at T = 2.0−10.0 K and H = 0−8.0 T.

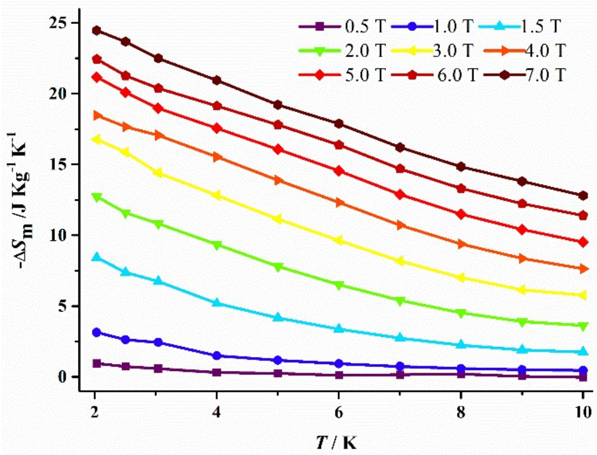

Fig. 5 Temperature dependence of magnetic entropy change ($-\Delta S_m$) as calculated from the magnetization data of **2** at T = 2.0−10.0 K and 0−7.0 T.

Table 2 Comparison of $-\Delta S_m$ values among cluster **2** and some reported Gd_4 clusters.

Gd_4 Clusters	**Magnetic interaction**	**$-\Delta S_m$ (J kg^{-1} K^{-1}) (ΔH)**	**ref**
Cluster **2**	AF	24.46 (7 T)	This work

View Article Online
DOI: 10.1039/D0NJ01969K

$[Gd_4(L)_2(dbm)_6(CH_3OH)_2]$	AF	21.39 (5 T)	33a
$[Gd_4(L)_2(dbm)_6(C_2H_5OH)_2]$	AF	20.26 (7 T)	33a
$[Gd_4(dbm)_4L_6(\mu_3\text{-}OH)_2]\cdot 5CH_3CN\cdot 0.5CH_2Cl_2$	AF	17.77 (7 T)	33b
$[Gd_4(acac)_4L_6(\mu_3\text{-}OH)_2]\cdot 2CH_3CN$	AF	22.11 (7 T)	33b
$[Gd_4(acac)_4L_6(\mu_3\text{-}OH)_2]\cdot CH_3CN\cdot 0.5CH_2Cl_2$	AF	25.08 (7 T)	33c
$[Gd_4(dbm)_4(L)_6(\mu_3\text{-}OH)_2]\cdot 5CH_3CN$	AF	16.35 (7 T)	33d
$[Gd_4(acac)_4L_6(\mu_3\text{-}OH)_2]$	AF	20.8 (7 T)	33e
$[Gd_4(acac)_4(\mu_3\text{-}OH)_2(L)_6]\cdot 4CH_3CN$	AF	23.37 (7 T)	33f
$[Gd_4(\mu_3\text{-}OH)_2L_6(acac)_4]\cdot 2CH_3CN$	AF	18.85 (7 T)	34a
$\{[Gd_4(L)_6(pbd)_4(\mu_3\text{-}OH)_2]\cdot 2CH_3CN\}$	AF	21.42 (7 T)	34b
$[Gd_4(L)_6(tmhd)_4(\mu_3\text{-}OH)_2]$	AF	20.85 (7 T)	34c
$[Gd_4(\mu_3\text{-}OH)_2(tmhd)_4L_6]\cdot 2CH_3CN$	AF	17.94 (7 T)	34d
$[Gd_4(\mu_3\text{-}OH)_2L_6(acac)_4]\cdot 2.5CH_3CN$	AF	19.39 (7 T)	34e
$[Gd_4(\mu_3\text{-}OH)_2L_6(tmhd)_4]\cdot CH_3CN\cdot CH_3CH_2OH$	AF	16.21 (7 T)	34e
$[Gd_4(CO_3)\ (L)_4(acac)_2(H_2O)_4]\cdot 2CH_3CN$	AF	31.23 (7 T)	34f
$[Gd_4CO_3L_4(acac)_2(MeOH)_2(H_2O)_2]\cdot MeOH\cdot H_2O$	AF	27.06 (7 T)	34f
$[Gd_4(HL)_4(\mu_2\text{-}CH_3O)_4]\cdot 4CH_3OH$	AF	34.46 (7 T)	35a
$[Gd_4(acac)_6L_2(CH_3O)_2(CH_3OH)_4]$	AF	27.96 (7 T)	35b
$[Gd_4(HL)_4(\mu_2\text{-}CH_3O)_4]\cdot 4CH_3OH$	AF	29.0 (7 T)	35c
$[Gd_4(\mu_3\text{-}OH)_4(L)_4(\mu_2\text{-}piv)_4(MeOH)_4]$	AF	25.57 (7 T)	35d
$[Gd_4(\mu_3\text{-}OH)_2(L)_2L_1L_2(HOCH_3)_2]\cdot 11H_2O$	AF	27.2 (7 T)	35e

In order to probe the magnetic relaxation dynamics of the Dy_4 cluster **4**, the alternating-current (*ac*) magnetic susceptibility measurements were performed as a function of the temperature on polycrystalline samples under zero *dc* magnetic field with an ac oscillating field of 3.0 Oe (Fig. 6). Both in-phase (χ') and out-of-phase (χ'') of **4** become frequency dependent and occurrence of two distinct peaks for the out-of-phase *ac* signals (χ'') is evident during the frequency range 911 Hz to 2311 Hz, indicating the possible occurrence of a multiple relaxation process. Such a behavior has been described in recent reported Dy_4 clusters and has been attributed to the occurrence

View Article Online
DOI: 10.1039/D0NJ01969K

of two different Dy^{III} coordination environment in **4**.[36] During the low frequency region 111 and 511 Hz, only one peak for the out-of-phase *ac* signals (χ'') was observed, and a rising tail was occurred during 8.0-2.0 K, indicate the presence of quantum tunneling effect (QTM) in **4**.[37]

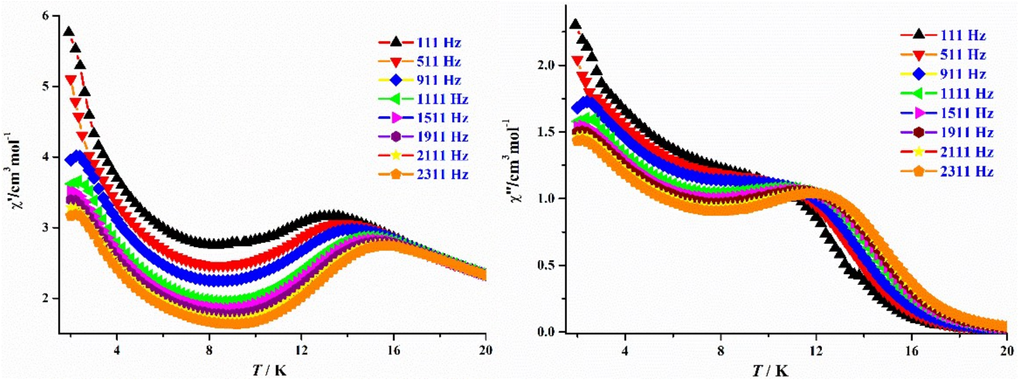

Fig. 6 Temperature dependence of in-phase (χ') and out-of-phase (χ'') components of the *ac* magnetic susceptibility under zero *dc* field for **4**.

The frequency dependencies of the *ac* susceptibility were measured under the zero dc fields to further explore the SMMs behaviors of cluster **4**. As show in Fig. 7, both the in-phase (χ') and out-of-phase (χ'') signals of the ac susceptibility of **4** show temperature dependencies, which further indicate the presence of slow relaxation of the magnetization in cluster **4**.[38] Because of the strong overlap of peaks at low temperatures, the evaluation of the effective energy barriers ($\Delta E/k_B$) for magnetization reversal and relaxation times has been possible only for the high-temperature feature. The relaxation time τ data of **4** derived from the out-of-phase (χ'') peaks in the form of lnτ plotted as a function of $1/T_P$ (Fig. 8). The relaxation time τ data obey the Arrhenius law $\tau = \tau_0 \exp(\Delta E/k_BT)$ at high-temperature range.[39] The best fitting results give the energy barriers $\Delta E/k_B$ = 75.0 K and the pre-exponential factor $\tau_0 = 1.57\times10^{-7}$ s. The $\Delta E/k_B$ value of cluster **4** obtained is higher than or comparable to these of other tetranuclear dysprosium complexes based on 8-hydroxyquinoline Schiff base and β-diketionate ligands, smaller than those of some Dy$_4$ clusters reported in the literature.[40] The τ_0 of the cluster **4** is consistent with the reported value of 10^{-6}-10^{-12} s for Dy-based clusters SMMs.[41]

View Article Online
DOI: 10.1039/D0NJ01969K

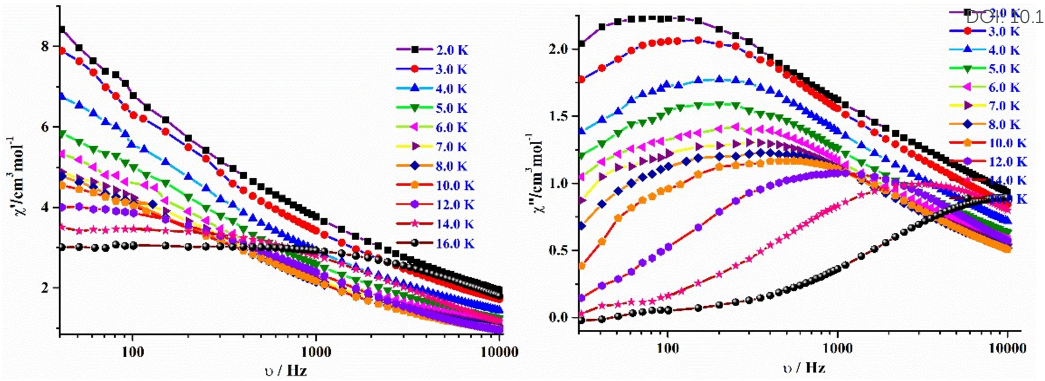

Fig. 7 Frequency dependence of in-phase (χ') and out-of-phase (χ'') components of the *ac* magnetic susceptibility under zero *dc* field for **4**.

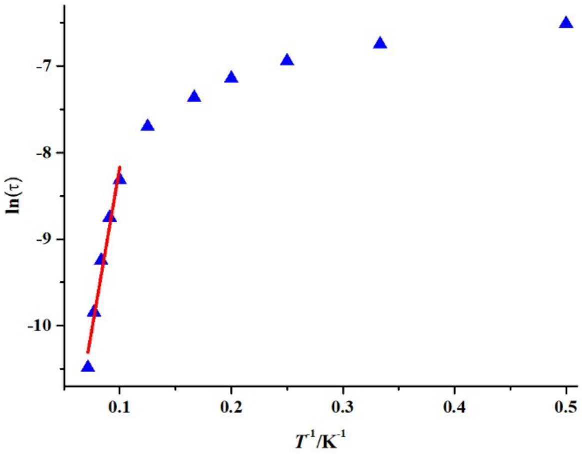

Fig. 8 Plot of ln(τ) vs. T^{-1} for **4** obtained under zero *dc* field, and the red line represents the Arrhenius fitted result.

As shown in Fig. 9, the Cole–Cole plots of χ'' *vs.* χ' for cluster **4** show nearly semi-circle shapes and the generalized Debye model was employed to fit these data.[42] The best fitted parameter α = 0.16-0.58 for **4** was obtained. The relatively large distribution coefficients α of cluster **4** indicate that there is a wide distribution of relaxation time in cluster **4**.

View Article Online
DOI: 10.1039/D0NJ01969K

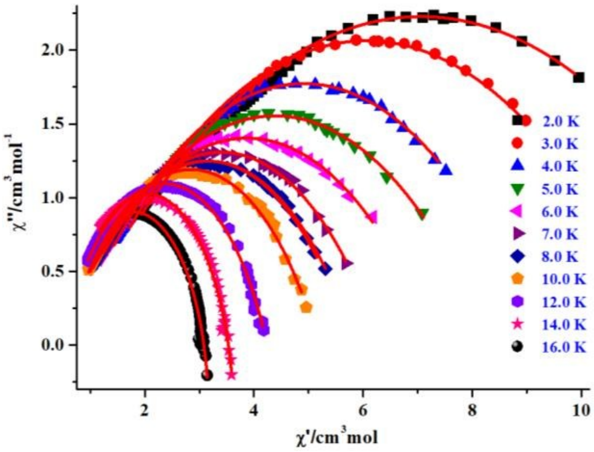

Fig. 9 Cole−Cole plots for **4** at zero *dc* field at the indicated temperatures. The solid lines indicate the best fits to the experiments with the generalized Debye model.

Conclusion

In conclusion, we have successfully synthesized five polynuclear lanthanide compounds with {Ln^{III}_4} cores, which show rhombus-shaped arrangement. The magnetic investigation reveal that Gd_4 cluster **2** displays cryogenic magnetocaloric effects with maximum $-\Delta S_m$ value of 24.46 J kg^{-1} K^{-1} at 2.0 K and ΔH = 7.0 T. It is a relatively larger magnetic entropy change ($-\Delta S_m$) value among the reported Gd_4 clusters based on 8-hydroxyquinoline Schiff base ligand. Whereas the tetranuclear Dy(III)-based cluster **4** shows single-molecule magnet (SMM) behavior with multiple magnetic relaxation processes. The energy barriers ($\Delta E/k_B$) of **4** are 75.0 K and τ_0 = 1.57×10^{-7} s.

Conflicts of interest

There are no conflicts to declare.

Acknowledgment

This work was supported financially by the National Natural Science Foundation of China (21571138), the Scientific and Technological Innovation Programs of Higher Education Institutions in Shanxi (No. 201802099), the Fund for Shanxi “1331 Project” Key Innovative Research Team, Key Laboratory of Ecological Restoration of Water Pollution (Taiyuan Normal University).

Notes and references

1 (a) Y. Z. Zheng, G. J. Zhou, Z. Zheng, R. E. P. Winpenny, *Chem. Soc. Rev*., 2014, **43**, 1462; (b) J. B. Peng, X. J. Kong, Q. C. Zhang, M. Orendač, J. Prokleška, Y. P. Ren, L. S. Long, Z. P. Zheng, and L. S. Zheng, *J. Am. Chem. Soc.*, 2014, **136**, 17938.

2 (a) H. L. Sun, Z. M. Wang and S. Gao, *Coord. Chem. Rev*.,2010, **254**, 1081; (b) P. Zhang, Y. N. Guo and J. K. Tang, Coord. Chem. Rev.,2013, **257**, 1728; (c) K. L. M. Harriman, J. L. Brosmer, L. Ungur, P. L. Diaconescu and M. Murugesu, *J. Am. Chem. Soc*., 2017, **139**, 1420; (d) S. W. Zhang and P. Cheng, *Chem Rec*., 2016, **16**, 2077; (e) S. W. Zhang, W. Shi and P. Cheng, Coord. *Chem. Rev*., 2017, **352**, 108; (f) S. J. Liu, S. D. Han, J. P. Zhao, J. Xu and X. H. Bu, *Coord. Chem. Rev.*, 2019, **394**, 39.

3 (a) P. Mahata, S. K. Mondal, D. K. Singha and P. Majee, *Dalton Trans*., 2017, **46**, 301; (b) H. Xu, C. S. Cao, X. M. Kang and B. Zhao, *Dalton Trans.*, 2016, **45**, 18003; (c) J. Y. Zou, L. Li, S. Y. You, Y. W. Liu, H. M. Cui, J. Z. Cui and S. W. Zhang, *Dalton Trans*., 2018, **47**, 15694.

4 (a) H. Xu, B. Zhai, C. S. Cao and B. Zhao, *Inorg. Chem*., 2016, **55**, 9671; (b) T. Q. Song, J. Dong, A. F. Yang, X. J. Che, H. L. Gao, J. Z. Cui and B. Zhao, *Inorg. Chem*., 2018, **57**, 3144; (c) Z. L. Wu, X. W. Lan, Y. X. Zhang, M. Li and G. Y. Bai, *Dalton Trans***.**, 2019, **48**, 11063.

5 (a) A. L. Dearden, S. Parsons and R. E. P Winpenny, *Angew. Chem., Int. Ed*., 2001, **40**, 151; (b) E. I. Tolis, M. Helliwell, S. Langley, J. Raftery and R. E. P. Winpenny, *Angew. Chem., Int. Ed*., 2003, **42**, 3804; (c) J. K. Tang, I. Hewitt, N. T. Madhu, G. Chastanet, W. Wernsdorfer, C. E. Anson, C. Benelli, R. Sessoli and A. K. Powell, *Angew. Chem., Int. Ed*., 2006, **45**, 1729; (d) R. J. Blagg, C. A. Muryn, E. J. L. McInnes, F. Tuna and R. E. P. Winpenny, *Angew. Chem., Int. Ed*., 2011, **50**, 6530.

6 N. Ishikawa, M. Sugita, T. Ishikawa, S. Koshihara and Y. Kaizu, *J. Am. Chem. Soc.*, 2003, **125**, 8694.

7 (a) M. U. Anwar, L. K. Thompson, L. N. Dawe, F. Habib and M. Murugesu, *Chem. Commun*., 2012, **48**, 4576; (b)X. L. Li, J. F. Wu, J. K. Tang, B. L. Guennic, W. Shi and P. Cheng, *Chem. Commun*., 2016, **52**, 9570; (c) E. M. Pineda, Y. Lan, O. Fuhr, W. Wernsdorfer and M. Ruben, *Chem. Sci*., 2017, **8**, 1178; (d) M. U. Anwar, L. K. Thompson, L. N. Dawe, F. Habib and M. Murugesu, *Chem. Commun*., 2012, **48**, 4576; (e) W. B. Sun, B. L. Han, P. H. Lin, H. F. Li, P. Chen, Y. M. Tian, M. Murugesu and P. F. Yan, *Dalton Trans*., 2013, **42**, 13397; (f) S. K. Gupta,

T. Rajeshkumar, G. Rajaraman and R. Murugavel, *Chem. Sci.*, 2016, **7**, 5181; (g) J. Xiong, H. Y. Ding, Y. S. Meng, C. Gao, X. J. Zhang, Z. S. Meng, Y. Q. Zhang, W. Shi, B. W. Wang and S. Gao, *Chem. Sci.*, 2017, **8**, 1288;(h) S. K. Gupta, T. Rajeshkumar, G. Rajaraman and R. Murugavel, *Chem. Sci.*, 2016, **7**, 5181.

8 (a) S. Bala, G. Z. Huang, Z. Y. Ruan, S. G. Wu, Y. Liu, L. F. Wang, J. L. Liu and M. L. Tong, *Chem. Commun.*, 2019, **55**, 9939;(b)Y. Ma, Y. Q. Zhai, Y. S. Ding, T. Han and Y. Z. Zheng, *Chem. Commun.*, 2020, **56**, 3979; (c) F. S. Guo, B. M. Day, Y. C. Chen, M. L. Tong, A. Mansikkamäki, and R. A. Layfield, *Angew. Chem., Int. Ed.*, 2017, **56**, 68.

9 J. Liu, Y. C. Chen, J. L. Liu, V. Vieru, L. Ungur, J. H. Jia, L. F. Chibotaru, Y. Lan, W. Wernsdorfer, S. Gao, X. M. Chen and M. L. Tong, *J. Am. Chem. Soc.*, 2016, **138**, 5441.

10 Y. S. Ding, N. F. Chilton, R. E. P. Winpenny and Y. Z. Zheng, *Angew. Chem., Int. Ed.*, 2016, **55**, 16071.

11 F S. Guo, B. M. Day, Y. C. Chen, M. L. Tong, A. Mansikkamäki, R. A. Layfield, *Science.*, 2018, **362**, 1400.

12 J. K. Tang, I. Hewitt, N. T. Madhu, G. Chastanet, W. Wernsdorfer, C. E. Anson, C. Benelli, R. Sessoli, and A. K. Powell, *Angew. Chem., Int. Ed.*, 2006, **45**, 1729.

13 (a) S. Shen, S. F. Xue, S. Y. Lin, L. Zhao and J. K. Tang, *Dalton Trans.*, 2013, **42**, 10413; (b) S. F. Xue, L. Zhao, Y. N. Guo, X. H. Chen and J. K. Tang, *Chem. Commun.*, 2012, **48**, 7031; (c) X. L. Li, J. F. Wu, J. K. Tang, B. L. Guennic, W. Shi and P. Cheng, *Chem. Commun.*, 2016, **52**, 9570.

14 J. L. Liu, Y. C. Chen, F. S. Guo and M. L. Tong, *Coord. Chem. Rev.*, 2014, **281**, 26.

15 Y. C. Chen, L. Qin, Z. S. Meng, D. F. Yang, C. Wu, Z. D. Fu, Y. Z. Zheng, J. L. Liu, R. Tarasenko, M. Orendáč, J. Prokleška, V. Sechovský and M. L. Tong, *J. Mater.Chem. A.*, 2014, **2**, 9851.

16 (a) K. Wang, Z. L. Chen, H. H. Zou, S. H. Zhang, Y. Li, X. Q. Zhang, W. Y. Sun and F. P. Liang, *Dalton Trans.*, 2018, **47**, 2337; (b) R. Y. Wang, H. D. Selby, H. Liu, M. D. Carducci, T. Z. Jin, Z. P. Zheng, J. W. Anthis and R. J. Staples, *Inorg. Chem.*, 2002, **41**, 278; (c) K. Wang, Z. L. Chen, H. H. Zou, K. Hu, H. Y. Li, Z. Zhang, W. Y. Sun and F. P. Liang, *Chem. Commun.*, 2016, **52**, 8297; (d) A. S. R. Chesman, D. R. Turner, B. Moubaraki, K. S. Murray, G. B. Deacon, and S. R. Batten, *Dalton Trans.*, 2012, **41**, 10903.

View Article Online
DOI: 10.1039/D0NJ01969K

17 J. B. Peng, X. J. Kong, Q. C. Zhang, M. Orendáč, J. Prokleška, Y. P. Ren, L.S. Long, Z. P. Zheng and L.S. Zheng, *J. Am. Chem. Soc.*, 2014, **136**, 17938.

18 J. Dong, P. Cui, P. F. Shi, P. Cheng and B. Zhao, *J. Am. Chem. Soc.*, 2015, **137**, 15988.

19 W. B. Sun, P. F. Yan, S. D. Jiang, B. W. Wang, Y. Q. Zhang, H. F. Li, P. Chen, Z. M. Wang and S. Gao, *Chem. Sci.*, 2016, **7**, 684.

20 (a) H. L. Gao, L. Jiang, S. Liu, H. Y. Shen, W. M. Wang and J. Z. Cui, *Dalton Trans.*, 2016, **45**, 253; (b) H. L. Gao, N. N. Wang, W. M. Wang, H. Y. Shen, X. P. Zhou, Y. X. Chang, R. X. Zhang and J. Z. Cui, *Inorg. Chem. Front.*, 2017,**4**, 860; (c) H. L. Gao, X. P. Zhou, Y. X. Bi, H. Y. Shen, W. M. Wang, N. N. Wang, Y. X. Chang, R. X. Zhang and J. Z. Cui, *Dalton Trans.*, 2017, **46**, 4669.

21 S. Katagiri, Y. Tsukahara, Y. Hasegawa and Y. Wada, *Bull. Chem. Soc. Jpn.*, 2007, **80**, 1492.

22 C. Caris, P. Baret, J. L. Pierre and G. Serratrice, *Tetrahedron.*, 1996, **52**, 4659.

23 E. A. Boudreaux and L. N. Mulay (Eds.), Theory and Applications of Molecular Paramagnetism, Wiley-Interscience, *New York*, 1976.

24 (a) G. M. Sheldrick, SHELXS-97, Program for the Solution of Crystal Structures, University of Göttingen, Germany, 1997; (b) G.M. Sheldrick, SHELXL-97, Program for the Refinement of Crystal Structures, University of Göttingen, Germany, 1997.

25 (a) A. K. Mondal, H. S. Jena, A. Malviya and S. Konar, *Inorg. Chem.*, 2016, **55**, 5237; (b) J. Liu, Y. C. Chen, Z. X. Jiang, J. L. Liu, J. H. Jia, L. F. Wang, Q. W. Li and M. L. Tong, *Dalton Trans.*, 2015, **44**, 8150; (c) D. Zhang, Y. M. Tian, W. B. Sun, H. F. Li, P. Chen, Y. Q. Zhang and P. F. Yan, *Dalton Trans.*, 2016, **45**, 2674; (d) A. Gusev, R. Herchel, I. Nemec, V. Shul'gin, I. L. Eremenko, K. Lyssenko, W. Linert and Z. Trávníček, *Inorg. Chem.*, 2016, **55**, 12470; (e) A. K. Jami, V. Baskar and E. C. Sanudo, *Inorg. Chem.*, 2013, **52**, 2432; (f) W. M. Wang, X. Y. Hu, Y. Yang, J. Q. Zhao, Y. X. Zhang, X. M. Kang and Z. L. Wu, *New J. Chem.*, 2020, **44**, DOI:10.1039/D0NJ01830A.

26 (a) S. Swavey and R. Swavey, *Coord. Chem. Rev.*, 2009, **253**, 2627; (b) Z. Ahmed and K. Iftikhar, *Inorg. Chim. Acta*, 2012, **392**, 161.

27 (a) H. S. Wang, B. Zhao, B. Zhai, W. Shi, P. Cheng, D. Z. Liao and S. P. Yan, *Cryst. Growth Des.*, 2007, **7**, 1851; (b) J. Xia, B. Zhao, H. S. Wang, W. Shi, Y. Ma, H. B. Song, P. Cheng, D.

View Article Online
DOI: 10.1039/D0NJ01969K

Z. Liao and S. P. Yan, *Inorg. Chem.*, 2007, **46**, 3450.

28 (a) Y. L. Hou, G. Xiong, B. Shen, B. Zhao, Z. Chen and J. Z. Cui, *Dalton Trans.*, 2013, **42**, 3587; (b) W. M. Wang, W. Z. Qiao, H. X. Zhang, S. Y. Wang, Y. Y. Nie, H. M. Chen, Z. Liu, H. L. Gao, J. Z. Cui, B. Zhao, *Dalton Trans.*, 2016, **45**, 8182.

29 (a) W. T. Xu, Y. F. Zhou, D. C. Huang, W. Xiong, M. Y. Su, K. Wang, S. Han and M. C. Hong, *Cryst. Growth Des.*, 2013, **13**, 5420; (b) W. M. Wang, H. X. Zhang, S. Y. Wang, H. Y. Shen, H. L. Gao, J. Z. Cui and B. Zhao, *Inorg. Chem.*, 2015, **54**, 10610.

30 (a) K. H. Zangana, E. M. Pineda and R. E. P. Winpenny, *Dalton Trans.*, 2014, **43**, 17101; (b) Y. L. Hou, G. Xiong, P. F. Shi, R. R. Cheng, J. Z. Cui and B. Zhao, *Chem. Commun.*, 2013, **49**, 6066; (c) W. M. Wang, S. Y. Wang, H. X. Zhang, H. Y. Shen, J. Y. Zou, H. L. Gao, J. Z. Cui and B. Zhao, *Inorg. Chem. Front.*, 2016, **3**, 133; (d) W. M. Wang, H. H. Liu, L. T. He, X. R. Han, Z. L. Wu, Y. G. Ran, J. Y. Zou and M. Fang, *Polyhedron.*, 2017, **133**, 119.

31 (a) M. Evangelisti, A. Candini, A. Ghirri, M. Affronte, E. K. Brechin and E. J. L. McInnes, *Appl. Phys. Lett.*, 2005, **87**, 072504; (b) M. Manoli, R. D. L. Johnstone, S. Parsons, M. Murrie, M. Affronte, M. Evangelisti and E. K. Brechin, *Angew. Chem., Int. Ed.*, 2007, **46**, 4456.

32 (a) L. X. Chang, G. Xiong, L. Wang, P. Cheng and B. Zhao, *Chem. Commun.*, 2013, **49**, 1055; (b) J. D. Leng, J. L. Liu and M. L. Tong, *Chem. Commun.*, 2012, **48**, 5286; (c) S. J. Liu, C. Cao, S. L. Yao, T. F. Zheng, Z. X. Wang, C. Liu, J. S. Liao, J. L. Chen, Y. W. Li and H. R. Wen, *Dalton Trans.*, 2017, **46**, 64; (d) S. J. Liu, C. Cao, C. C. Xie, T. F. Zheng, X. L. Tong, J. S. Liao, J. L. Chen, H. R. Wen, Z. Chang and X. H. Bu, *Dalton Trans.*, 2016, **45**, 9209; (e) T. F. Zheng, S. L. Yao, C. Cao, S. J. Liu, H. K. Hu, T. Zhang, H. P. Huang, J. S. Liao, J. L. Chen and H. R. Wen, *New J. Chem.*, 2017, **41**, 8598; (f) S. J. Liu, T. F. Zheng, J. Bao, P. P. Dong, J. S. Liao, J. L. Chen, H. R. Wen, J. Xu and X. H. Bu, *New J. Chem.*, 2015, **39**, 697; (g) T. F. Zheng, X. M. Tian, L. H. Wu, S. J. Liu, S. L. Yao, K. H. He, H. Huang, J. Liao, J. L. Chen and H. R. Wen, *New J. Chem.*, 2019, **43**, 18445.

33 (a) Y. C. Zhang, Q. L. Wang, G. Chen, P. F. Shi and W. M. Wang, Polyhedron., 2019, **169**, 247; (b) H. L. Gao, N. N. Wang, W. M. Wang, H. Y. Shen, X. P. Zhou, Y. X. Chang, R. X. Zhang and J. Z. Cui, *Inorg. Chem. Front.*, 2017, **4**, 860; (c) H. L. Gao, X. P. Zhou, Y. X. Bi, H. Y. Shen, W. M. Wang, N. N. Wang, Y. X. Chang, R. X. Zhang and J. Z. Cui, *Dalton Trans.*, 2017, **46**, 4669; (d) H. L. Gao, S. X. Huang, X. P. Zhou, Z. Liu and J. Z. Cui, *Dalton Trans.*, 2018, **47**, 3503; (e) H. L. Gao, L. Jiang, S. Liu, H. Y. Shen, W. M. Wang and J. Z.

View Article Online
DOI: 10.1039/D0NJ01969K

Cui, *Dalton Trans.*, 2016, **45**, 253; (f) W. M. Wang, L. Zhang, X. Z. Li, L. Y. He, X. X. Wang, Y. Shi, J. Wang, J. Dong and Z. L. Wu, *New J. Chem.*, 2019, **43**, 12941.

34(a) W. M. Wang, T. L. Han, Y. L. Shao, X. Y. Qiao, Z. L. Wu, Q. L. Wang, P. F. Shi, H. L. Gao and J. Z. Cui, *New J. Chem.*, 2018, **42**, 14949; (b) H. Yu, J. X. Yang, J. Q. Han, P. F. Li, Y. L. Hou, W. M. Wang and M. Fang, *New J. Chem.*, 2019, **43**, 8067; (c) M. Fang, L. J. Shao, T. X. Shi, Y. Y. Chen, H. Yu, P. F. Li, W. M. Wang and B. Zhao, *New J. Chem.*, 2018, **42**, 11847; Y. X. Zhang, Y. H. Zhang, B. Y. Liu, W. M. Wang, G. P. Tang, H. Y. Wei and Z. L. Wu, *New J. Chem.*, 2018, **42**, 18305; (e) Y. X. Zhang, M. Li, B. Y. Liu, Z. L. Wu, H. Y. Wei and W. M. Wang, *RSC Adv*., 2017, **7**, 55523; (f) W. M. Wang, Z. L. Wu, Y. X. Zhang, H. Y. Wei, H. L. Gao and J. Z. Cui, *Inorg. Chem. Front.*, 2018, **5**, 2346.

35 (a) W. M. Wang, X. Z. Li, L. Zhang, J. L. Chen, J. H. Wang, Z. L. Wu and J. Z. Cui, *New J. Chem.*, 2019, **43**, 7419; (b) W. M. Wang, L. Y. He, X. X. Wang, Y. Shi, Z. L. Wu and J. Z. Cui, *Dalton Trans.*, 2019, **48**, 16744; (c) W. M. Wang, M. J. Wang, S. S. Hao, Q. Y. Shen, M. L. Wang, Q. L. Liu, X. F. Guan, X. T. Zhang and Z. L. Wu, *New J. Chem.*, 2020, **44**, 4631; (d) A. Rasamsetty, C. Das, E. C. Sañudo, M. Shanmugam and V. Baskar, *Dalton Trans.*, 2018, **47**, 1726; (e) J. A. Sheikh, A. Adhikary and S. Konar, *New J. Chem*., 2014, **38**, 3006.

36 (a) Y. N. Guo, G. F. Xu, P. Gamez, L. Zhao, S. Yan Lin, R. P Deng, J. K. Tang and H. J. Zhang *J. Am. Chem. Soc.*, 2010, **132**, 8538; (b) V. Chandrasekhar, S. Hossain, S. Das, S. Biswas and J. P. Sutter, *Inorg. Chem.*, 2013, **52**, 6346.

37 (a) Y. Peng, V. Mereacre, A. Baniodeh and A. K. Power, *Inorg. Chem.*, 2016, 55, 68; (b) J. A. Sheikh, A. Adhikary and S. Konar, *New J. Chem.*, 2014, 38, 3006.

38 (a) S. D. Jiang, B. W. Wang, G. Su, Z. M. Wang and S. Gao, *Angew. Chem., Int. Ed.*, 2010, **49**, 7448; (b) S. D. Jiang, B. W. Wang, H. L. Sun, Z. M. Wang and S. Gao, *J. Am. Chem. Soc.*, 2011, **133**, 4730; (c) S. W. Zhang, H. Li, E. Y. Duan, Z. S. Han, L. L. Li, J. K. Tang, W. Shi and P. Cheng, *Inorg Chem.*, 2016, **5**5, 1202.

39 (a) P. H. Lin, T. J. Burchell, L. Ungur, L. F. Chibotaru, W. Wernsdorfer and M. Murugesu, *Angew. Chem. Int. Ed*., 2009, **48**, 9489; (b) J. Liu, Y. C. Chen, Z. X. Jiang, J. L. Liu, J. H. Jia, L. F. Wang, Q. W. Li and M. L. Tong, *Dalton Trans.*, 2015, **44**, 8150; (c) T. Lacelle, G. Brunet, A. Pialat, R. J. Holmberg, Y. Lan, B. Gabidullin, I. Korobkov, W. Wernsdorfer and M. Murugesu, *Dalton Trans.*, 2017, **46**, 2471.

View Article Online
DOI: 10.1039/D0NJ01969K

40 (a) H. L. Gao, L. Jiang, W. M. Wang, S. Y.Wang, H. X. Zhang and J. Z. Cui, *Inorg. Chem.*, 2016, **55**, 8898; (b) Z. L. Wu, Y. G. Ran, X. Y. Wu, Y. P. Xia, M. Fang, W. M. Wang, *Polyhedron*, 2017, **126**, 282; (c) R. X. Zhang, Y. X. Chang, H. Y. Shen, W. M. Wang, X. P. Zhou, N. N. Wang, J. Z. Cui and H. L. Gao, *Dalton Trans.*, 2016, **45**, 19117; (d) W. M. Wang, X. Y. Zhao, H. Qiao, L. Bai, H. F. Han, M. Fang, Z. L. Wu and J. Y. Zou, *Journal of Solid State Chemistry*., 2017, **253**, 154; (e) Y. L. Wang, C. B. Han, Y. Q. Zhang, Q. Y. Liu, C. M. Liu and S. G. Yin, *Inorg. Chem.*, 2016, **55**, 5578; (f) Q. Chen, F. Ma, Y. S. Meng, H. L. Sun, Y. Q. Zhang and Song Gao, *Inorg. Chem.*, 2016, **55**, 12904.

41 (a) P. Zhang, L. Zhang, C. Wang, S. F. Xue, S. Y. Lin and J. K. Tang, *J. Am. Chem. Soc.*, 2014, **136**, 4484; (b) S. F. Xue, X. H. Chen, L. Zhao, Y. N. Guo and J. K. Tang, *Inorg. Chem.*, 2012, **51**, 13264; (c) H. Q. Tian, L. Zhao, Y. N. Guo, Y. Guo, J. K. Tang and Z. L. Liu, *Chem. Commun.*, 2012, **48**, 708; (d) N. Ishii, Y. Okamura, S. Chiba, T. Nogami and T. Ishida, *J. Am. Chem. Soc.*, 2008, **130**, 24; (e) K. S. Gavrilenko, O. Cador, K. Bernot, P. Rosa, R. Sessoli, S. Golhen, V. V. Pavlishchuk and L. Ouahab, *Chem. – Eur. J.*, 2008, **14**, 2034.

42 (a) S. M. J. Aubin, Z. Sun, L. Pardi, J. Krzystek, K. Folting, L. C. Brunel, A. L. Rheingold, G. Christou and D. N. Hendrickson, *Inorg. Chem.*, 1999, **38**, 5329; (b) K. S. Cole and R. H. Cole, *J. Chem. Phys.*, 1941, **9**, 341.

View Article Online
DOI: 10.1039/D0NJ01969K

Table of contents

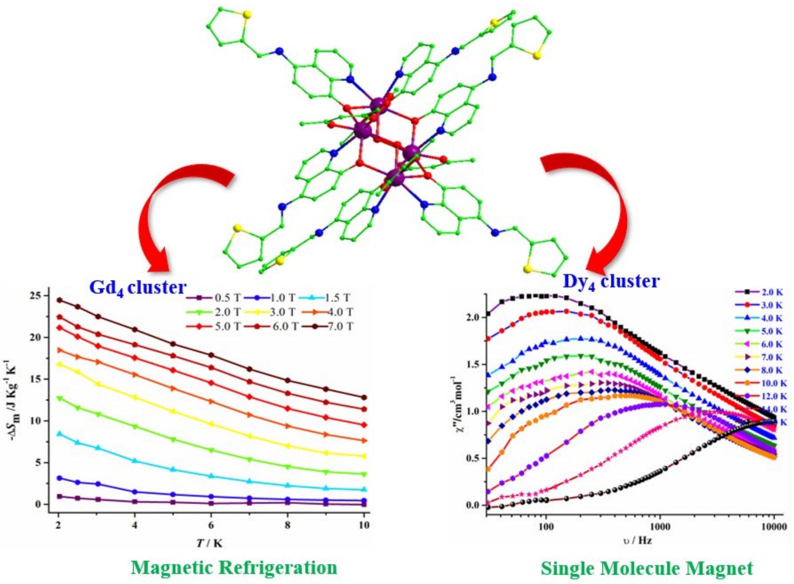

Rhombus-shaped Gd_4 cluster displays magnetic refrigeration property, and Dy_4 cluster shows remarkable SMMs behaviors .